13th ewtec 2019 Proceedings of the 13th European Wave and Tidal Energy Conference 1-6 Sept 2019, Naples, Italy

Peak-shaving control – a new control paradigm for OWC wave energy converters

João C.C. Henriques, Ana A.D. Carrelhas, Luís M.C. Gato, António F.O. Falcão, Juan C.C. Portillo, and J. Varandas

***Abstract*—The OWC (oscillating water column) is a class of wave energy converters (WECs) whose power take-off system typically comprises a turbine/generator set. Since its introduction in 2011, the biradial self-rectifying air turbine has set a new performance level against all other turbines for this type of applications. The biradial turbine designed and constructed within the framework of the ongoing European project H2020 OPERA is expected to contribute to further improve the OWC technology through the use of a high-speed safety valve (HSSV) installed in series with the turbine. The HSSV can be used, not only for phase control – latching – but notably also for peak-shaving control. Peak-shaving can be achieved by performing real-time control of the valve position to limit the available power to the turbine. This power constraint allows decreasing the generator rated power, the WEC operation under more energetic sea states without overloading the generator, increasing the capacity factor of the wave energy converter and improving the quality of the electrical energy supplied to the grid. The contribution of the paper is the introduction of a new nonlinear feedback control algorithm to adjust the valve position as a function of the rotational speed. The proposed control algorithm was calibrated and tested at the new IST 55 kW variable-flow turbine test rig with a 30 kW biradial air turbine-generator prototype. Results presented demonstrate the effectiveness of the control under simulated oscillating flow induced by irregular waves.**

***Keywords* — wave energy, oscillating water column, peak shaving control, peak-to-average power ratio control.**

I. Introduction

THE ocean waves are a potential source of unexploited renewable energy. Despite the extensive research & development programmes of the last 40 years, all wave energy converters prototypes failed to reach the commercial stage. There are several reasons for the unsuccesses, but the most obvious ones are closely related to the randomness and the large peak-to-average ratio of the ocean waves resource. Under storm situations, the typical peak-to-average power ratio of the ocean waves can range from 50 to 100, and these values provide extreme conditions for mechanical design. In normal operating conditions, the peak-to-average ratio is considerably lower, ranging from 7 to 10, thus mainly affecting the design and operation of the power take-off (PTO) system, as the power plant is expected to be shut down for safety purposes in wave storms. Besides, most of the PTO systems do not handle with high-efficiency the typical peak-to-average ratio found in wave energy converters.

The hydrodynamic performance and the integration of the PTO system, especially under extreme wave conditions are critical issues [1]–[4]. Yet few works have been devoted to the integrated study of the hydrodynamics and the power take-off system under these conditions.

For grid operators, the integration of this form of renewable energy - the wave energy with its unique specific features - introduces new challenges that have to be addressed. In most devices, peak-to-average power ratio control - peak shaving - is a difficult task due to the limited capability of the power take-off system to control or dissipate the excess of energy that occurs in the more energetic sea states.

Normal operation under medium to more energetic sea states requires a PTO system with an oversized generator. This choice has two main drawbacks: a) it increases the PTO costs and, most importantly, b) it reduces the produced energy due to the inherent low efficiency of the generator/power converter set under small load operation.

The oscillating-water-column (OWC) devices are possibly the systems in which the control of the peak-to-average power ratio can be more easily and more effectively achieved. In an OWC, there is a fixed or floating hollow structure, open to the sea below the water surface, that traps air above the inner free-surface [5]. Wave action alternately compresses and decompresses the trapped air which is forced to flow through a turbine coupled to a generator. The PTO of an OWC device has only one moving part: an air turbine/generator set installed above the water level. The typical turbine rotational speed is in the range of 500-2000 rpm allowing the use of commercial off-the-shelf electrical generators from two- to eight pairs of poles [6]. These configurations reduce the manufacture, installation and maintenance costs.

The safe operation of the PTO system requires the

This paper, with ID 1421, has been submitted in the EWTEC 2019 conference track *Grid integration, power take-off and control*. This research was partially supported by: i) FCT (Foundation for Science and Technology), Portugal, through IDMEC (Institute of Mechanical Engineering), under LAETA, project UID/EMS/ 50022/2019; ii) European Union's Horizon 2020 research and innovation programme under grant agreement No 654444 (OPERA Project); and iii) WAVEBUOY project - Wave-powered oceanographic buoy for long-term deployment - PTDC/MAR-TEC/0914/2014. The first author was funded by FCT researcher grant No. IF/01457/2014.

J.C.C. Henriques (e-mail: joaochenriques@tecnico.ulisboa.pt), A.A.D. Carrelhas (e-mail: ana.carrelhas@tecnico.ulisboa.pt), L.M.C. Gato (e-mail: luis.gato@tecnico.ulisboa.pt), A.F.O. Falcão (e-mail: antonio.falcao@tecnico.ulisboa.pt), and J.C.C. Portillo (e-mail: juan.portillo@tecnico.ulisboa.pt) are at IDMEC, Instituto Superior Técnico, Universidade de Lisboa, Av. Rovisco Pais, 1049-001 Lisboa, Portugal

J. Varandas (e-mail: jose.varandas@kymaner.com) is at Kymaner - Tecnologias Energéticas, Lda., Estrada do Paço do Lumiar, Campus do Lumiar, Edif. D R/C, Sala 1026, Lisboa, Portugal

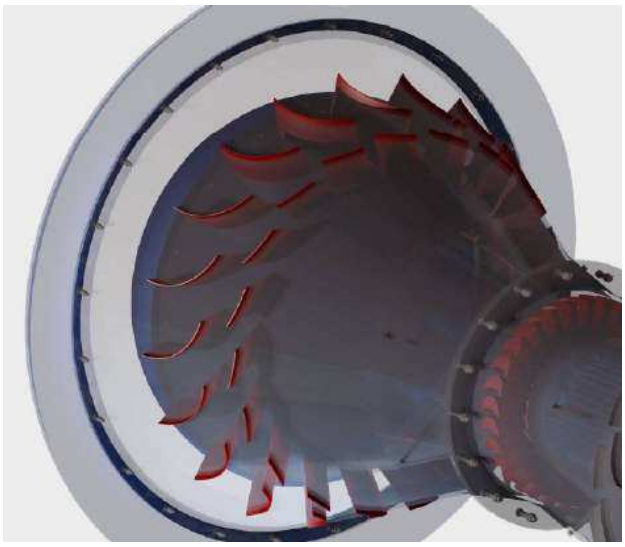

Fig. 1. Topology of the guide-vane system of the Kymaner self-rectifying axial-flow impulse turbine (reproduced from [7].

limitation of the pneumatic power available to the turbine. Two valve configurations can be used to control the turbine flow rate: a) a relief valve installed in parallel with the turbine or b) a high-speed safety valve (HSSV) mounted in series with the turbine. The relief valve is a very appealing concept. However, the large size required for the valve has deterred its application. Apart from PTO protection, the HSSV may have another application: the so-called latching control.

The wave energy harvesting technology is still far from the maturity level of the wind and photovoltaic sectors [8], [9]. The EU has recognised this fact has provided several policy mechanisms to raise the competitiveness of the wave energy industry to the level of the more conventional renewable technologies [1]. The OPERA project has received funding from the European Union's Horizon 2020 research and innovation programme to collect, analyse and share open-sea operating data and experience (http://opera-h2020.eu/). The near-term goal is to validate and de-risk several industrial innovations for wave energy, taking them from a laboratory environment (TRL 3) to a marine environment (TRL 5). On the long run, consortium expects to contribute to a cost reduction of over 50% on the price of the produced electricity.

One of the goals of the OPERA project was the design, construction and real sea trials of a biradial turbine with 30 kW. The biradial turbine designed for the project is of a second generation with an improved stator, comprising two sets of fixed guide vanes arranged into concentric annular rows, and a new high-speed valve. The new stator is an evolution of the stator proposed in 2009 for an axial impulse turbine [7], see Fig. 1.

The biradial turbine overcomes several limitations of the first generation of self-rectifying air turbines for OWC devices. The turbine is symmetrical with respect to a mid-plane perpendicular to its axis of rotation, see Fig. 2. A pair of radial-flow guide-vane rows surround the rotor blades. Each guide vane row is connected to the rotor by an axisymmetric duct whose walls are flat discs. The unique geometry of the biradial turbine allows an axially sliding mechanism that operates as an HSSV with a typical stroke of less than 10% of the turbine diameter. Although latching control introduces an increased mechanical complexity in the system, it has been found that appropriate control of the turbine flow could reduce the overall system costs by decreasing the size of the device for the same extracted power.

The biradial turbine has the unique feature of having a built-in HSSV installed in series with the rotor. The HSSV can operate in three modes: a) safety valve - a slow on/off mode aiming to control the turbine rotational speed, b) latching valve - for phase control and c) high-speed peak-shaving which is the object of the present study.

Theoretically, an HSSV can also be installed in Wells or axial-flow impulse turbines. In this type of turbines, the HSSV must close a large annular duct in a short time interval which is a tough engineering challenge. Salter [10] proposed a sophisticated pneumatic valve to close the annular duct of the 1.7 m diameter Wells turbine of the Pico plant within the required actuation time. The practical complexity of this type of valves is probably the main reason why, until recently, very few papers were published on OWC latching control [11]–[15].

In oscillating-body wave energy converters (WECs), dynamic forces resulting from latching or peak-shaving control must be withstood by the PTO system or by some additional braking system, see Fig. 4. In the case of stiff systems, such as hydraulic circuits or linear generators, this may be seen as a major structural problem especially for dynamic compressive stresses (buckling). Peak power control or latching under medium to more energetic sea state conditions aggravate these difficulties. Furthermore, the cyclic nature of the wave forces induces significant fatigue and wear problems. The control algorithm may try to alleviate the structural stresses by applying for the latching/peak-shaving order only when the (relative) velocity of the floater with respect to the PTO system is close. However, this approach introduces an undesired phase lag in the response.

The compressibility of the air in the chamber of an OWC plays an essential role in the design and operation of the WEC for several reasons:

- Changes the system response phase.
- Reduces the impact forces and fatigue problems, increases the system reliability and, most importantly, decreases structural costs.
- It decreases the forces resulting from peak-shaving/latching since a) the area of the valve surface subject to the chamber pressure is a small fraction of the area of the OWC free surface and b) the air compressibility has a spring effect.
- Allows applying peak-shaving/latching whenever it is required. Removes the constraint of operating the HSSV in the instant of zero relative velocity between the floater and the OWC.
- Latching is not so effective as in the case of an oscillating rigid body WEC since closing the HSSV does not stop the relative motion between the inner free-surface and the structure (spring effect).

Another component of the PTO system that may increase the overall efficiency with peak-shaving con-

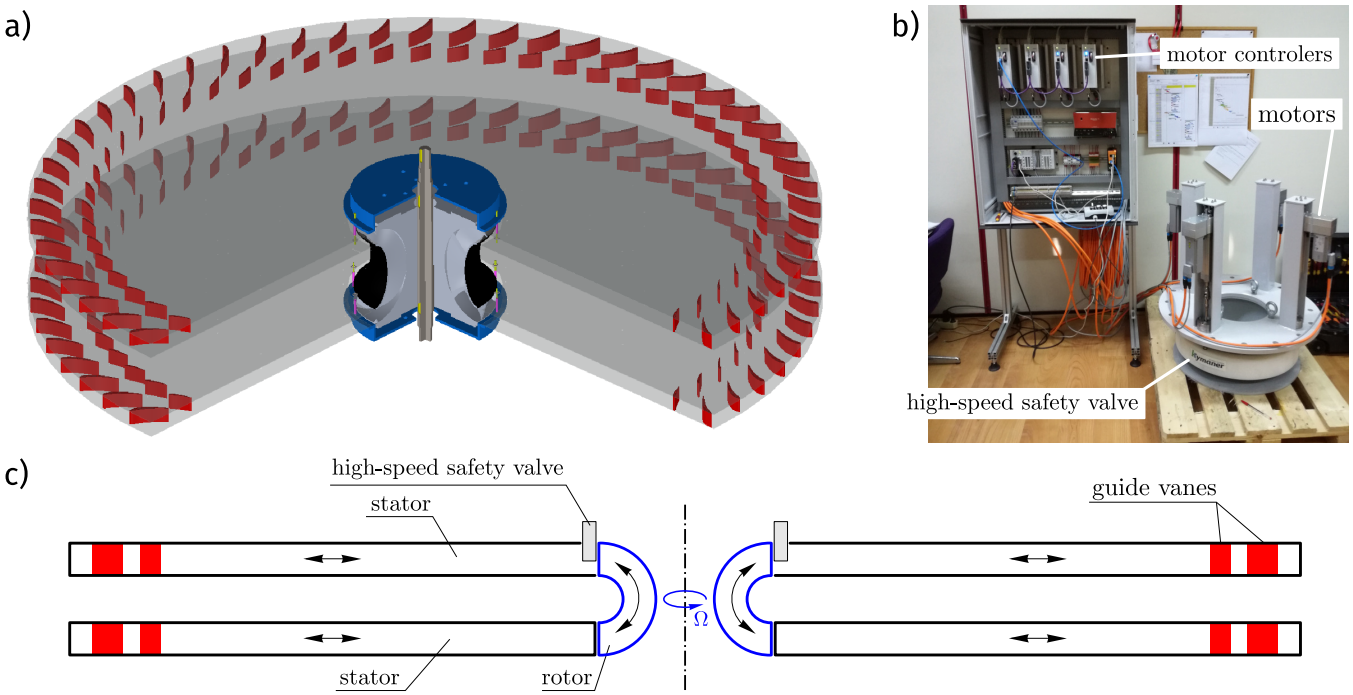

Fig. 2. a) Three-dimensional view of the biradial turbine. b) Peak shaving valve during reliability tests. c) Meridional cut of the turbine showing the average velocity direction when the flow is from the atmosphere to the air chamber.

Fig. 3. Biradial turbine installed at the IST variable-flow turbine test rig.

trol is the electrical generator. Electrical generators are known to perform poorly at partial loads less than about one-third of the rated power. Besides, overheating of the power electronics prevents the rated power from being exceeded. Air turbines behave differently. If their rotational speed is adequately controlled, they can work close to the optimum operating point for a very wide range of load conditions.

The focus of the present work is to limit the maximum available power to the PTO system by using a peak-shaving control algorithm that controls instantaneously the position of the HSSV installed in series with the turbine. Peak-shaving is simple and effective control since it is a throttling process (a pressure loss in a valve).

This strategy reduces the required rated power of the generator/converter set and increases the power output of the system. The algorithm was tested and validated experimentally with a 30 kW biradial air turbine-generator prototype in the variable flow turbine test rig of IST [16], Fig. 3.

The paper is organised as follows. Section II presents the general methodology used to described the turbine performance. The proposed peak-shaving control algorithm is presented in Section III. The turbine test rig used in the experimental setup is characterised in Section IV. Section V reports the turbine performance curves under partial valve closure. The real-time implementation of the peak-shaving control algorithm is detailed in Section VI. Experimental results are reported in section VII. Conclusions can be found in section VIII.

II. Turbine characterization

The performance characteristics of air turbines can be presented as dimensionless functions of only the dimensionless pressure head Ψ, for Reynolds numbers typically

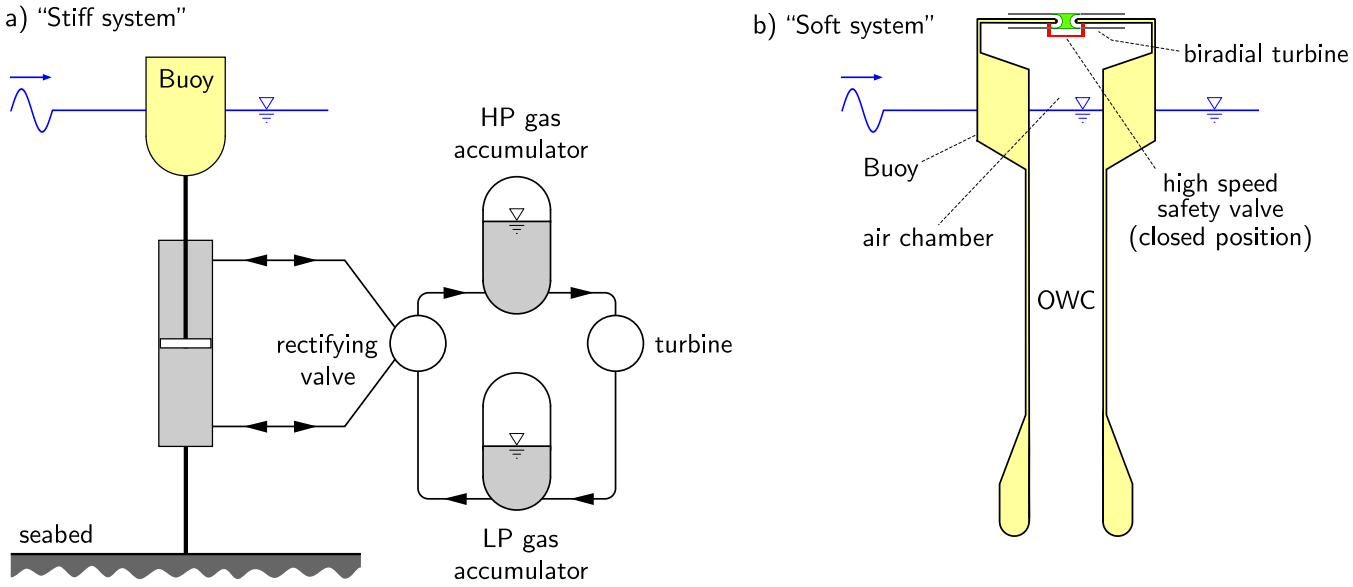

Fig. 4. a) A point absorber wave energy converter based in an hydraulic system equipped with hig-pressure and low-pressure gas accumulators to mitigate the peak-to-average power ratio. b) A floating OWC spar-buoy wave energy converter equipped with a biradial turbine.

greater than $\mathrm{Re} = \Omega D^2/\nu > 10^6$ and low Mach numbers $\mathrm{Ma} = \Omega D/c_{\mathrm{in}} < 0.3$ [17], [18]. As such, we find that

$$\Phi = f_\Phi(\Psi), \tag{1}$$

$$\Pi = f_\Pi(\Psi), \tag{2}$$

where

$$\Psi = \frac{\Delta p}{\rho_{\mathrm{in}}\,\Omega^2\,D^2}, \tag{3}$$

$$\Phi = \frac{\dot{m}_{\mathrm{turb}}}{\rho_{\mathrm{in}}\,\Omega\,D^3}, \tag{4}$$

$$\Pi = \frac{P_{\mathrm{turb}}}{\rho_{\mathrm{in}}\,\Omega^3\,D^5}. \tag{5}$$

Here Φ is the dimensionless flow rate, Π is the power coefficient, Δp is the stagnation pressure head, ρ_{in} is the inlet density at stagnation conditions, Ω is rotational speed, D is the turbine rotor diameter, $\dot{m}_{\mathrm{turb}}$ is the mass flow rate, and P_{turb} output aerodynamic power. The functions $f_\Pi(\Psi)$ and $\eta(\Psi)$ are even and the function $f_\Phi(\Psi)$ is odd.

The turbine efficiency measures the ratio between output aerodynamic power over the available pneumatic power

$$\eta_{\mathrm{turb}} = \frac{P_{\mathrm{turb}}}{P_{\mathrm{pneu}}} = \frac{\Pi}{\Phi\,\Psi} = \frac{f_\Pi(\Psi)}{f_\Phi(\Psi)\,\Psi}, \tag{6}$$

where $P_{\mathrm{pneu}} = \Delta p\, Q_{\mathrm{turb}}$, and $Q_{\mathrm{turb}} = \dot{m}/\rho_{\mathrm{in}}$ is the turbine volumetric flow rate at inlet conditions.

The dynamics of the turbine/generator set is given by

$$\frac{\mathrm{d}}{\mathrm{d}t}\left(\tfrac{1}{2} I\Omega^2\right) = P_{\mathrm{turb}} - P_{\mathrm{ctrl}}, \tag{7}$$

where I and P_{ctrl} are the moment of inertia of the rotating parts and the instantaneous generator electromagnetic power imposed to control the rotational speed.

The turbine aerodynamic power is computed from Eq. (5)

$$P_{\mathrm{turb}} = \rho_{\mathrm{in}}\,\Omega^3 D^5\, f_\Pi(u\Psi). \tag{8}$$

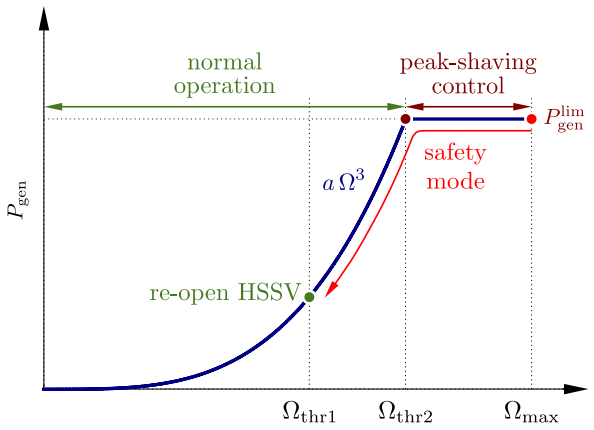

Fig. 5. Non-linear generator control law with HSSV partial closing.

Here it is assumed that a safety valve is installed in series with the turbine. The control variable $u \in [0, 1]$ represents the position of the HSSV the controller, where $u = 0$ and $u = 1$ denotes the closed and the open positions, respectively.

The mass flow rate is computed analogously as

$$\dot{m}_{\mathrm{turb}} = \rho_{\mathrm{in}}\,\Omega D^3\, f_\Phi(u\Psi). \tag{9}$$

III. Peak-Shaving control algorithm

To derive a simple and effective generator control law, let us consider the limiting case when the inertia I is zero. Under this condition, the instantaneous torque transmitted at the generator shaft is equal to the instantaneous electromagnetic torque, Eq. (7). To maximise efficiency, the turbine must operate at the best efficiency point (bep), Ψ_{bep}. The turbine power is proportional to

$$P_{\mathrm{turb}}\,(\Psi_{\mathrm{bep}}, \Omega) = \underbrace{\rho_{\mathrm{in}}\,D^5\, f_\Pi(u\Psi_{\mathrm{bep}})}_{a_{\mathrm{bep}} \approx \mathrm{const}}\,\Omega^3, \tag{10}$$

where a_{bep} can be assumed constant in a first approximation since the variations of the density ρ_{in} are small

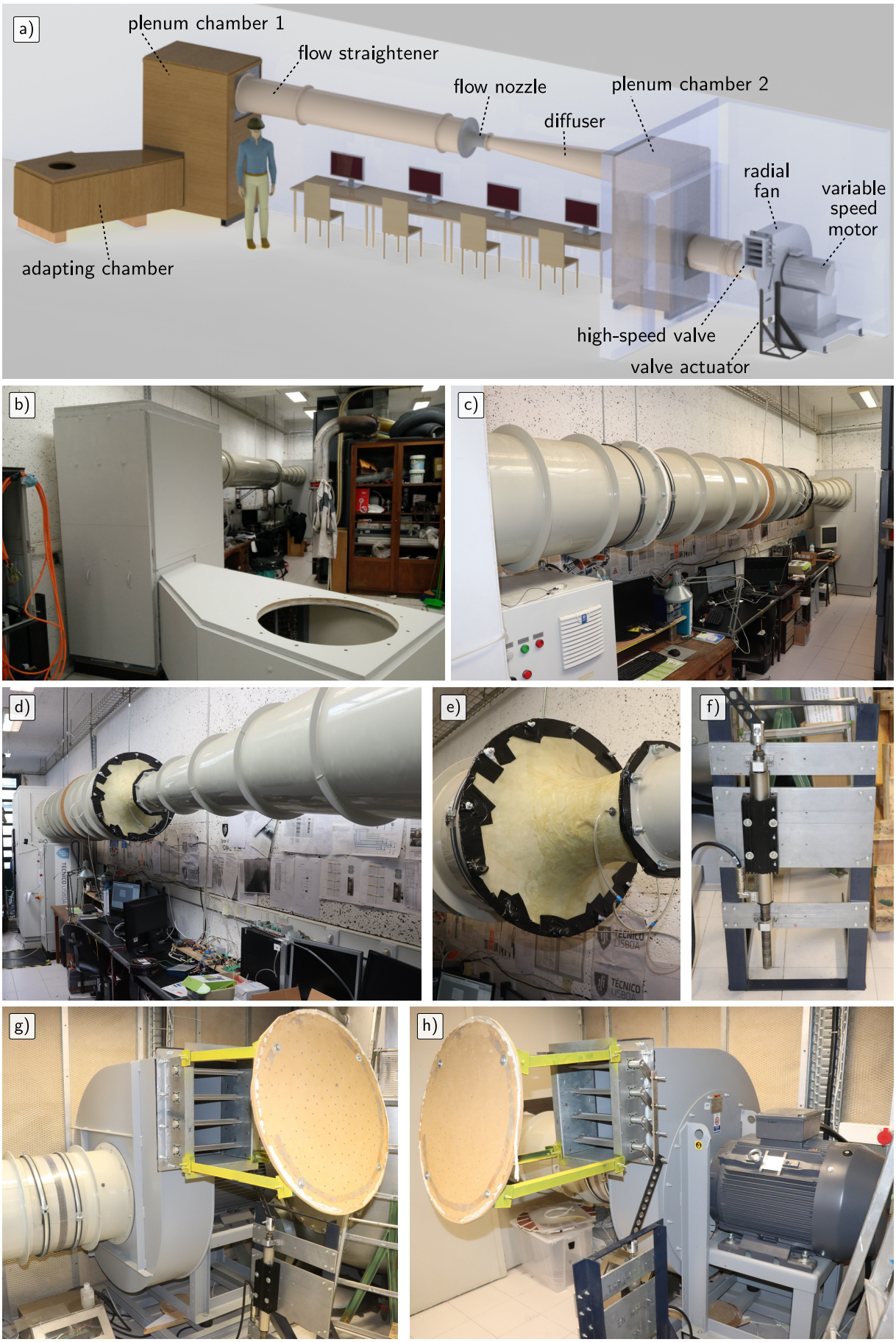

Fig. 6. a) General overview of the IST variable-flow test rig without turbine. Details of: b) adapting chamber and plenum chamber 1, c) flow straightener, d) flow nozzle and diffuser, e) flow nozzle, f) valve actuator, g) radial fan, high-speed valve and valve actuator, and f) radial fan, high-speed valve and variable-speed motor. In g) and h) it is also depicted a damping plate used to dissipate the energy of the jet that exits from the high-speed valve.

TABLE I
MAIN CHARACTERISTICS OF THE IST VARIABLE-FLOW TEST RIG WITHOUT THE TURBINE INSTALLED.

Parameter	Value	Units
Max. flow rate	4.0	[m^3/s]
Max. gauge pressure, Δp	12.0	[kPa]
Min. valve closing time	0.4	[s]
Max. wave frequency, $f_{\max}$	1.5	[Hz]

in comparison with the changes of the rotational speed. As such, a generator power control law can be defined as

$$P_{\text{ctrl}} = a_{\text{bep}}\Omega^3, \tag{11}$$

to maximize the turbine power output.

In practice, we can use a general relationship of the type [19]

$$P_{\text{ctrl}} = a\,\Omega^b. \tag{12}$$

where b is expected to have values around 3.

In the present work, we propose a more sophisticated control law as shown in Fig. 5. Under normal operation, $0 \le \Omega \le \Omega_{\text{thr2}}$ the control algorithm applies Eq. (12). If the threshold Ω_{thr2} is exceeded, the valve is closed within the range $1.0 \ge u \ge 0.4$ such that the generator power is kept constant. If the maximum rotational speed, $\Omega_{\max}$, is exceeded, the valve is closed and open when the rotational speed is lower than Ω_{thr1}. The HSSV positioning algorithm is described in section VI. The suction effect on the side of the valve exposed to the turbine flow rate imposes a vertical force that must be supported by the actuators. If the valve is kept in an almost closed position, the actuators need to do a considerable force. As such, to avoid the valve actuators overheating, the valve position was limited to $u = 0.4$.

IV. TEST-RIG DESCRIPTION

The variable flow test-rig was designed and constructed with the aim of testing self-rectified air turbines under steady and variable unidirectional air flows, Fig. 6. The unique feature of this test is the ability to accurately reproduce pressure spectra that are within the facility operating limits.

The core component of the facility is a high-speed air valve connected to a radial fan which drives the air through the turbine. The air valve consists of a multi-blade air damper operated by a 3-Phase linear electrical motor of 1024 N of maximum force. The linear motion of the motor's slider is converted into rotary motion of the valve's blades by a simple slider crank-chain mechanism. The test-rig flow capabilities are presented in Table I.

The test rig was designed to create negative gauge pressure downstream of the turbine. Therefore, the radial fan's inlet is connected on the downstream end of the duct system, see Fig. 6. On the other end of the duct-work, the turbine's inlet is open to the free atmosphere. The plenum chambers, the flow nozzle used to measure the flow rate and the diffuser were designed according to the AMCA 210-99 Standards for experimental turbine testing [20].

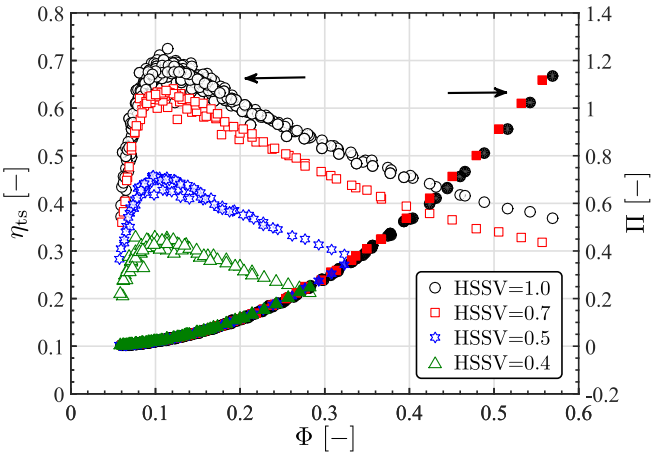

Fig. 7. Total-to-static efficiency and power coefficient as a function of the flow coefficient.

V. TURBINE PERFORMANCE UNDER PARTIALLY HSSV CLOSING

The characterisation of the turbine performance under conditions of partial closure of the HSSV is of major importance to perform peak-shaving control. As such, four valve filling positions, $u \in \{0.4, 0.5, 0.7, 1.0\}$, were studied and the respective operating curves were analysed.

The tests were carried out in the range of speeds $495 \le \Omega \le 2595$ rpm, corresponding to values of the Reynolds number of $2.1\times10^5 \le \text{Re} \le 1.3\times10^6$, and in the range of flow coefficients of $0.05 \le \Phi \le 0.56$.

Figure 7 depicts the efficiency curves of the prototype are given as a function of the flow coefficient for four positions of the HSSV, u. From Fig. 7 we found that the maximum efficency $\eta_{\text{turb}}^{\max} = 0.70$ occurs for $\Phi = 0.115$. As expected, the position u of the HSSV changes the turbine characteristics $\Psi(\Phi)$. The maximum efficiency of the turbine starts to present a large drop for $u < 0.7$, see Figs. 7 and 8. However, the efficiency curves have similar shapes. The behaviour of Fig. 8 is explained in Section VI.

The power coefficient curve has unexpected behaviour. The position of the valve changes the available dimensionless pressure head and, as a result, the dimensionless flow rate is given by a function, $\Phi = \tilde{f}_\Phi(u, \Psi)$, that does not depend only on Ψ, as in the case of Eq. (1).

Curiously, if we plot the power coefficient as a function of the flow rate the curve does not depend on the valve position u. This result, which is not very intuitive, indicates that the valve is locally modifying the flow, producing losses in the valve and the inlet of the rotor, but maintaining approximately the angular momentum of the flow at the inlet of the rotor. Therefore, the amount of energy per unit mass exchanged between the fluid and the rotor (the so-called E_{r}) remains approximately constant, despite the efficiency of the rotor decreases due to the incidence losses at the inlet of the rotor as a consequence of the acceleration of the flow in the valve. It should be recalled that the primary function of the valve in a partial closure position is to dissipate energy and not to maintain the performance of the turbine.

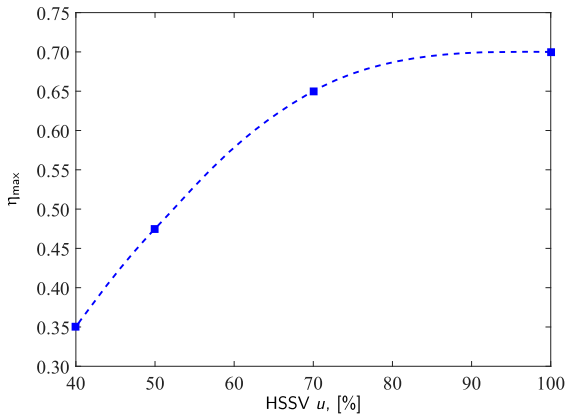

Fig. 8. Pressure coefficient as a function of the flow coefficient.

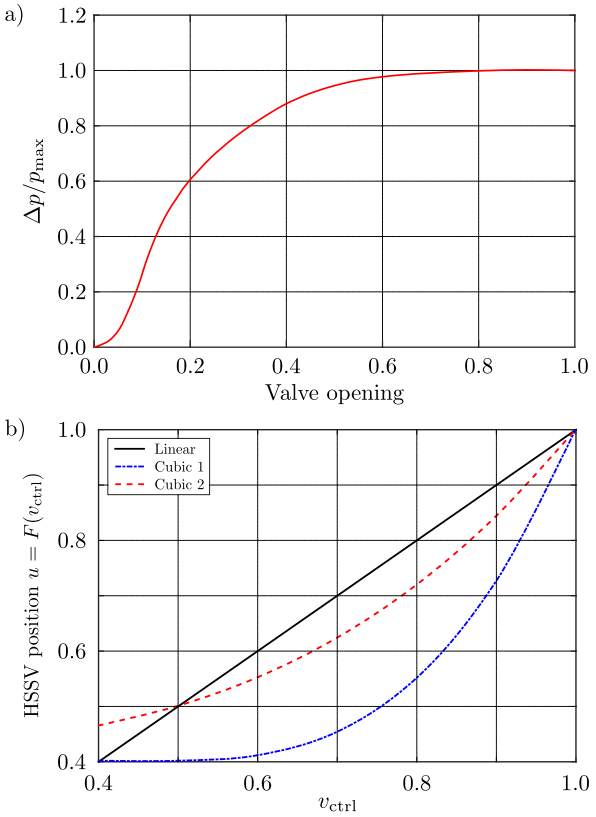

Fig. 9. a) Typical pressure drop across a valve as a function of the closure position. b) Auxiliary variable u_{ctrl} used to achieve a faster response of the pressure drop across the HSSV.

VI. Real-time implementation of the peak-shaving control

Peak-shaving control aims to limit the available power to the turbine in the region $\Omega_{\text{thr2}} \leq \Omega \leq \Omega_{\text{max}}$, see Fig. 5. The biggest challenge to devise an algorithm to perform peak-shaving control is to understand how the pressure drop is affected by the closure of the valve. Figure 9 a) shows a typical pressure drop across a valve as a function of the valve position. Initially, between 100% and 70% of the opening, the pressure drop is small. If the closing operation continuous then the slope of the pressure drop, as a function of the valve position, increases until the valve is almost closed.

In the present peak-shaving control algorithm, an intermediate function

$$u(v_{\text{ctrl}}) = F(v_{\text{ctrl}}), \tag{13}$$

was defined, and the closing position was assumed to be a function of a proportional controller defined as

$$v_{\text{ctrl}} = k_p \left(\Omega - \Omega_{\text{thr2}}\right), \tag{14}$$

where k_p is an empirical constant. The auxiliary function $F(v_{\text{ctrl}})$ aims to impose a more linear behaviour on the valve closure algorithm. The valve should close more in the initial stages and less when the slope of the pressure drop is higher. In the present work, a linear and two cubic functions were tested as candidates to the auxiliary function $F(v_{\text{ctrl}})$, see Fig. 9.

Figure 10 show the performance of the three curves considering that the generator power was limited to $P_{\text{gen}}^{\text{lim}} = 5\,\text{kW}$. As can be seen, cubic law 1 was the one that was able to have a tight control the generator power. The other functions were discarded because they fail to limit the generator power.

VII. Experimental results

The results of the generator power, rotational speed, HSSV position, as functions of time and two generator power limits $P_{\text{gen}}^{\text{lim}} \in \{2, 3\}\,\text{kW}$, resulting from the experimental tests at the IST variable-flow test rig are depicted in Fig. 11. The results show that the generator power was successfully limited in all tests. The oscillations of generator power around the imposed limits are small.

The case where $P_{\text{gen}}^{\text{lim}} = 3\,\text{kW}$, the valve positions varies from the fully opened to 40%, while for $P_{\text{gen}}^{\text{lim}} = 2\,\text{kW}$ the valve is constantly at the 40% open position. It is important to reinforce the idea that it was not necessary to close the valve completely in any test, once again validating the robustness of this control. For more energetic conditions, it may be necessary to close the valve for a longer period the reduce the rotational kinetic energy of the turbine/generator set.

VIII. Conclusions

The biradial turbine with a built-in sliding high-speed safety valve with accurate positioning opened to the possibility of controlling the excess of energy available to the turbine/generator set. In the present work, a new peak-shaving control algorithm for an OWC floating WEC was successfully implemented and tested in a large scale test rig connected to the power grid. The compressibility of the air in the OWC chamber allows the operation of the high-speed stop valve whenever required by the control algorithm, which is not possible for stiff systems like hydraulic PTOs or direct linear drive electrical generators. This possibility is one of the most significant advantages of OWC based devices in comparison with other types of WECs.

The proposed control algorithm was able to control the available power to the turbine such that the generator was never overloaded. The presented results also show that it is possible to reduce the generator peak-to-average power significantly. As such, it is possible to select a generator and power electronics with substantially small rated power. This selection will reduce the

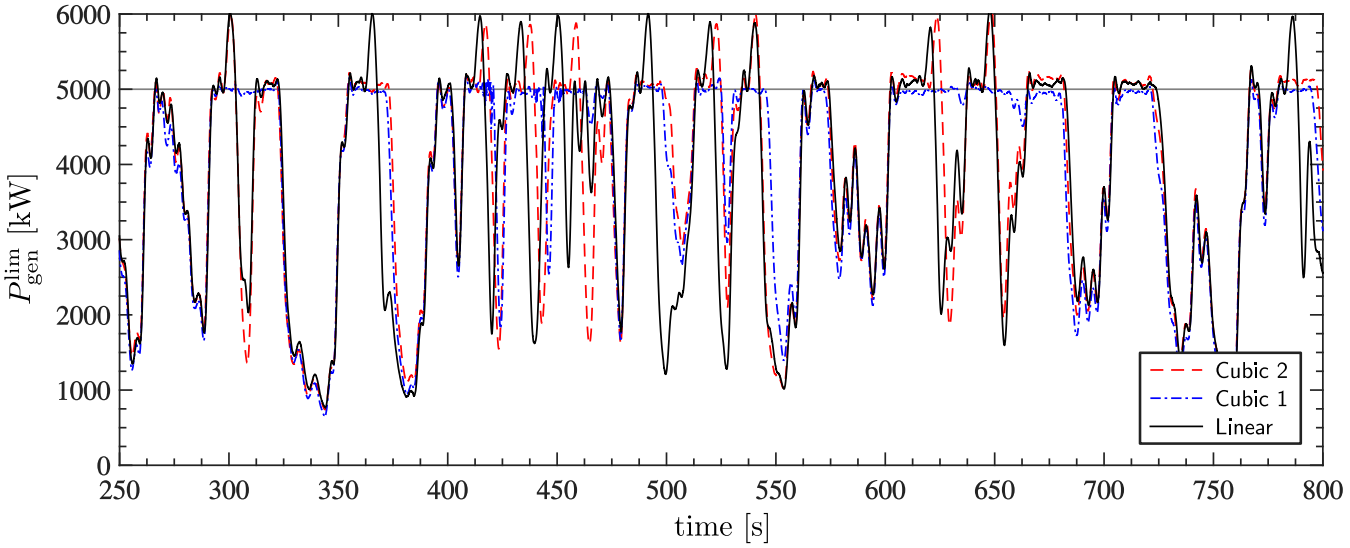

Fig. 10. Evaluation of the performance of the auxiliary functions $F(v_{\text{ctrl}})$. The generator power limit was set to $P_{\text{gen}}^{\text{lim}} = 5\,\text{kW}$.

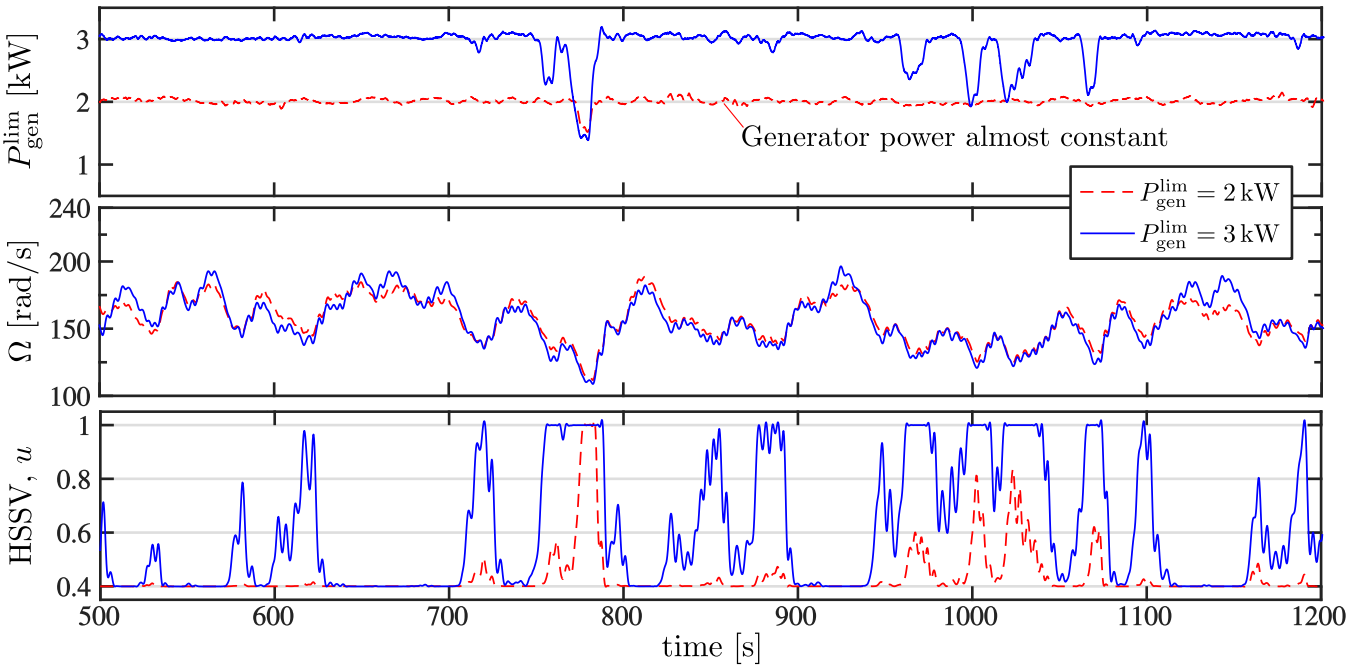

Fig. 11. Comparison of the behaviour of the peak-shaving algorithm with a generator power limit of 3 kW (blue/solid) against a more constrained generator power limit of 2 kW (red/dashed). The depicted time-series are of the generator power, rotational speed and HSSV position u, as functions of the time, considering the auxiliary function "Cubic 1".

PTO costs and increase the efficiency as the electrical components will always operate at larger mean loads.

IX. Conclusion

Two stators designs for a self-rectifying axial-flow air turbine were presented: the conventional design constituted by a single row of guide-vanes and the new design composed by three-rows of guide-vanes. Both stators were designed to produce a similar flow deflection angles. However, the system of three rows of guide-vanes presents a considerable smaller flow blockage at the exit stator which enables a significant reduction of the stagnation pressure loss in the flow through the exit stator and, consequently, it is expected to provide a significant increase of the turbine efficiency.

Preliminary results without the exit stator revealed that the efficiency reaches a peak of $\eta = 0.56$ for $\Phi = 0.12$, for the conventional design, and $\eta = 0.54$ for $\Phi = 0.11$, for the new design with three rows of guide-vanes. It was also observed that the flow angles at the inlet of the rotor correspond to the ones expected from the design: $\overline{\alpha}_2 = 74.3\,^\circ$ for the three-row stator and $\overline{\alpha}_2 = 71.9\,^\circ$ for the single row.

Despite the tests executed so far, we do not have enough results to justify the differences observed between the efficiencies of the two turbine models. Further work includes the measurement of the pressure and velocity radial distributions at the rotor exit and to allow the detailed analysis of the turbine losses for both cases, once the results indicate high kinetic energy losses at

the rotor exit. This work is in progress, and the results will be available at the time of the submission of the final version of the paper.

References

[1] D. Magagna and A. Uihlein, "Ocean energy development in europe: Current status and future perspectives," *International Journal of Marine Energy*, vol. 11, pp. 84 – 104, 2015.

[2] T. M. Ferguson, A. Fleming, I. Penesis, and G. Macfarlane, "Improving OWC performance prediction using polychromatic waves," *Energy*, vol. 93, Part 2, pp. 1943 – 1952, 2015.

[3] I. López, A. Castro, and G. Iglesias, "Hydrodynamic performance of an oscillating water column wave energy converter by means of particle imaging velocimetry," *Energy*, vol. 83, pp. 89 – 103, 2015.

[4] D.-Z. Ning, J. Shi, Q.-P. Zou, and B. Teng, "Investigation of hydrodynamic performance of an OWC (oscillating water column) wave energy device using a fully nonlinear HOBEM (higher-order boundary element method)," *Energy*, vol. 83, pp. 177 – 188, 2015.

[5] A. F. O. Falcão and J. C. C. Henriques, "Oscillating-water-column wave energy converters and air turbines: A review," *Renewable Energy*, vol. 85, pp. 1391 – 1424, 2016.

[6] D. O'Sullivan, "Electrical generators in ocean energy converters," in *Electrical design for ocean wave and tidal energy systems*, R. Alcorn and D. O'Sullivan, Eds. Stevenage: The Institution of Engineering and Technology, 2013, pp. 3–41.

[7] L. Trigo, "The OWC option," in *Workshop on Powering the Future? Marine Energy Opportunities, Lisbon*, 2009. [Online]. Available: http://www.wavec.org/eventos/marine_energy_2009#.WG-14dKLSos

[8] A. F. de O. Falcão, "Wave energy utilization: A review of the technologies," *Renewable and Sustainable Energy Reviews*, vol. 14, no. 3, pp. 899 – 918, 2010.

[9] R. Bucher and I. Bryden, "Overcoming the marine energy pre-profit phase: What classifies the game-changing "array-scale success"?" *International Journal of Marine Energy*, 2015.

[10] S. Salter and J. Taylor, "The design of a high-speed stop valve for oscillating water columns," in *Proc. 2nd European Wave Energy Conf.*, vol. 3, 1996, pp. 195–202.

[11] R. E. Hoskin and N. K. Nichols, "Latching control for a point absorber wave-power device," Department of Mathematics, University of Reading, Technical report NA1/86, 1986.

[12] R. E. Hoskin, B. M. Count, N. K. Nichols, and D. A. C. Nicol, "Phase control for the oscillating water column," in *IUTAM Symp. Hydrodynamics of Ocean-Wave Energy Utilisation*, D. V. Evans and A. F. O. Falcão, Eds. Springer-Verlag, 1986, pp. 257–268.

[13] R. Jefferys and T. Whittaker, "Latching control of an oscillating water column device with air compressibility," in *Hydrodynamics of Ocean Wave Energy Utilization*, D. V. Evans and A. F. de O. Falcão, Eds. Berlin: Springer-Verlag, 1986, pp. 281–291.

[14] P. A. P. Justino, "Pontryagin Maximum Principle and control of a OWC power plant," in *Proceedings of the 25st International Conference on Offshore Mechanics and Arctic Engineering*, Hamburg, Germany, 2006, pp. 65–73.

[15] J. C. C. Henriques, A. F. O. Falcão, R. P. F. Gomes, and L. M. C. Gato, "Latching control of an OWC spar-buoy wave energy converter in regular waves," in *Proceedings of the 31st International Conference on Offshore Mechanics and Arctic Engineering*, Rio de Janeiro, Brazil, 2012.

[16] F. X. C. da Fonseca, J. C. C. Henriques, L. M. C. Gato, and A. F. O. Falcão, "Oscillating flow rig for air turbine testing," *Submitted for publication in Renewable Energy (2018)*, 2018.

[17] S. L. Dixon and C. A. Hall, *Fluid mechanics and thermodynamics of turbomachinery*, 7th ed. Oxford: Butterworth-Heinemann, 2013.

[18] E. Dick, *Fundamentals of Turbomachines*, ser. Fluid Mechanics and Its Applications. Springer Netherlands, 2015, vol. 109.

[19] A. F. de O. Falcão, "Control of an oscillating-water-column wave power plant for maximum energy production," *Applied Ocean Research*, vol. 24, no. 2, pp. 73 – 82, 2002.

[20] *Laboratory Methods of Testing Fans for Aerodynamic Performance Rating*, Air Movement and Control Association International Inc, 1999, ANSI/AMCA 210-99 - ANSI/ASHRAE 51-1999. [Online]. Available: https://archive.org/details/gov.law.amca.210.1999